THE JOURNAL OF PHYSICAL CHEMISTRY Letters

Letter

pubs.acs.org/JPCL

Polymorphism of Crystalline Molecular Donors for Solution-Processed Organic Photovoltaics

Thomas S. van der Poll,[†] Andriy Zhugayevych,[‡] Eli Chertkov,[‡] Ronald C. Bakus, II,[†] Jessica E. Coughlin,[†] Simon J. Teat,[§] Guillermo C. Bazan,*[,†] and Sergei Tretiak*[,‡]

[†]Departments of Materials and Chemistry & Biochemistry, Center for Polymers and Organic Solids, University of California, Santa Barbara, California 93106, United States

[‡]Theoretical Division, Center for Nonlinear Studies and Center for Integrated Nanotechnologies, Los Alamos National Laboratory, T-12, MS B268, Los Alamos, New Mexico 87545, United States

[§]Advanced Light Source, Lawrence Berkeley National Laboratory, 6 Cyclotron Road, Berkeley, California 94720, United States

Supporting Information

ABSTRACT: Using ab initio calculations and classical molecular dynamics simulations coupled to complementary experimental characterization, four molecular semiconductors were investigated in vacuum, solution, and crystalline form. Independently, the molecules can be described as nearly isostructural, yet in crystalline form, two distinct crystal systems are observed with characteristic molecular geometries. The minor structural variations provide a platform to investigate the subtlety of simple substitutions, with particular focus on polymorphism and rotational isomerism. Resolved crystal structures offer an exact description of intermolecular ordering in the solid state. This enables evaluation of molecular binding energy in various crystallographic configurations to fully rationalize observed crystal packing on a basis of first-principle calculations of intermolecular interactions.

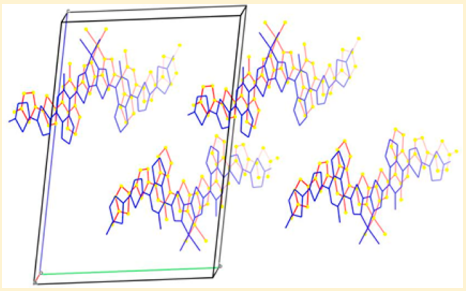

SECTION: Molecular Structure, Quantum Chemistry, and General Theory

Molecular design strategies for organic semiconducting chromophores revolve around established structure–property relationships.[1−8] The current design toolbox based on intuition, comparison against literature precedent, and computational approaches is primarily limited to insight on the molecular scale. Small changes at the molecular level may drive more substantial changes in bulk properties; many of which rely on the strength and type of intermolecular contacts.[9] There is therefore a need to better understand the impact of molecular connectivity on the meso and bulk scales, particularly in this context as molecular self-assembly plays a critical role in the operation of semiconducting devices.[10−13] The mechanism, by which subtle changes in chemical composition or processing conditions result in large changes in macroscopic properties, is polymorphism of molecular solids.[14−17] From a theoretical perspective, such polymorphism poses a challenge for crystal structure prediction and, ultimately, for establishing structure–property relationships.[18−20] In this contribution, we analyze four molecules using experimentally determined crystal structures and theoretical methods to elucidate key factors responsible for the high sensitivity of relevant macroscopic properties, such as charge transport and photogeneration of charge carriers, to small changes in chemical structure. From a practical perspective, such knowledge has the potential to deliver a predictive basis for the design of organic semiconductors.

Molecules **1**−**4**, shown in Chart 1, represent a class of molecules that have demonstrated excellent performance in solution-processed bulk-heterojunction solar cells.[21−23] This class of molecule adheres to an architecture generally described as donor−acceptor−donor−acceptor−donor, wherein disparate electronic character of adjacent building blocks gives rise to low energy charge transfer excited states and consequently narrow bandgaps. Single crystals were grown via solvent vapor

Chart 1. Molecules 1−4 in Their Optimized Geometry[a]

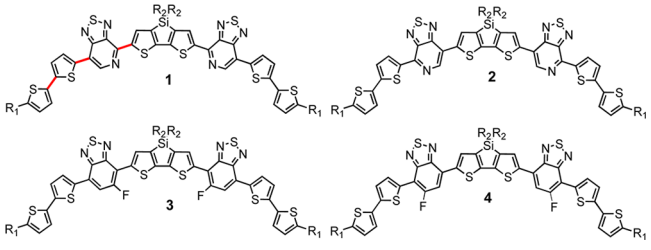

[a]R_1 = C_6H_{13}, R_2 = 2-ethylhexyl. Bold red bonds indicate location of dihedrals 1−3, from left to right, respectively.

Received: June 20, 2014
Accepted: July 22, 2014
Published: July 22, 2014

dx.doi.org/10.1021/jz5012675 | J. Phys. Chem. Lett. 2014, 5, 2700−2704

diffusion of molecules **1** and **3**,[24,25] and we report for the first time **4** and attempted unsuccessfully for molecule **2**. The geometry of the conjugated backbones (CBBs) for **1**−**4** chosen for illustration in Chart 1 is also the geometry of molecule **1** in its observed monoclinic crystal structure as well as one observed polymorph of **4**, in which static disorder reflects a partial population of **4** with a single inverted heterocycle. This class of molecules has been shown to typically crystallize in optimized geometries,[26] yet we observe a violation of this for two crystals; molecule **3** and a polymorph of **4** exhibit linear CBBs within a triclinic unit cell. There are no obvious steric or electrostatic explanations for this discrepancy considering that molecule **4** appears in each configuration in the experimentally determined lattices. Lattices structurally similar to crystal **1** will be referred to as type *a* (Figure 1a) and the lattice similar to

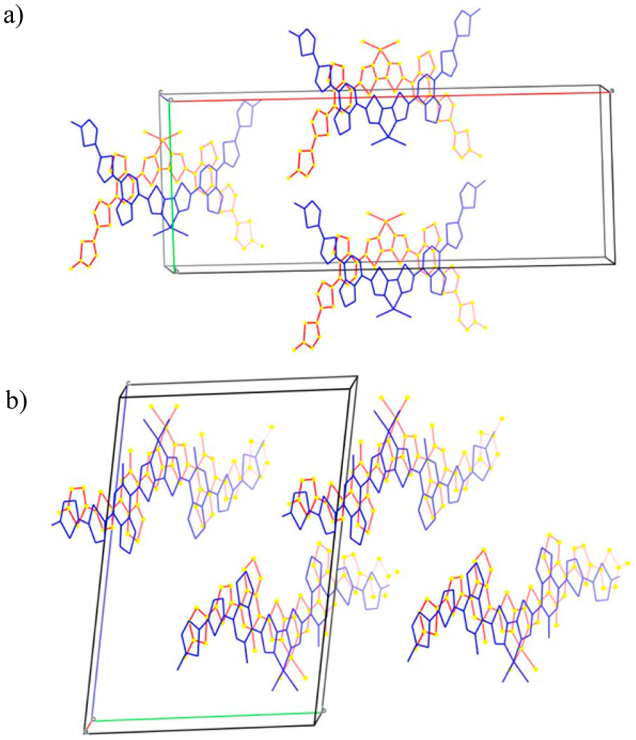

Figure 1. Truncated portions of experimentally determined crystal structures of **1** (a) and **3** (b) from a perspective parallel to π-stacks illustrating characteristic type *a* and type *b* lattices, respectively.

crystal **3** will be referred to as type *b* (Figure 1b). The molecular features we observe in resolved lattices that distinguish type *b* from type *a* are three flipped dihedrals in the CBB, as illustrated in Figure 1. Two implications that follow from these observations are (1) the significance of rotational isomerism and (2) the preferential formation of lattices comprising unoptimized geometries. While molecular shape is cited as an important facet of solid-state packing and ongoing efforts seek to control shape via connectivity and conformational locks,[27−34] neither of the aforementioned implications have been represented in molecular design strategies. To rationalize experimental observations, we have applied two distinct modeling approaches: density functional theory (DFT) and classical molecular mechanics (force field). The details of the computational methodology are given in the Supporting Information. For DFT calculations, we use CAM-B3LYP density functional combined with 6-31g* basis set. For classical molecular dynamics (MD), we use MM3 force field, which treats π-conjugated system quantum mechanically using Huckel Hamiltonian.

We start with the consideration of structural and electronic properties of molecules in solution, from which the bulk material is formed. Semiconducting molecules typically consist of tens to hundreds of atoms, including side chains. This results in a computationally prohibitive conformational space countable only by special techniques like replica exchange.[35] When studying extended π-conjugated systems using theoretical methods, most of the electronic properties of an isolated molecule are determined by the CBB.[36−39] For intramolecular electronic properties, this variety of conformations results only in some inhomogeneous broadening of observables such as IP/EA or peaks in optical spectra.[24] In contrast, intermolecular properties such as electronic couplings or structural arrangements are highly sensitive to variations in conformation of individual molecules as well as the nature of solubilizing side groups.

For **1**−**4**, the conformational analysis of CBBs has been performed on a DFT level. Here each CBB has six bonds that link aromatic units (bonds 1−6 moving along the CBB), and all six bonds possess a possibility of two planar configurations. Table 1 provides a concise summary of the energetic landscape

Table 1. Energetics of Rotational Isomerism[a]

mol.	env.[b]	E_p[c]	E_{f1}[d]	E_{f2}	E_{f3}	E_{b1}[e]	E_{b2}	E_{b3}
1	vac.	9	31	34	66	118	187	407
2	vac.	6	32	65	28	134	405	182
3	vac.	9	31	30	24	119	204	209
4	vac.	9	31	26	22	121	200	210
1	$CHCl_3$	8	27	13	65	123	159	361
2	$CHCl_3$	4	27	64	7	136	358	153
3	$CHCl_3$	8	27	6	17	125	173	171
4	$CHCl_3$	8	27	19	0	124	174	168

[a]All values are in units of millielectronvolts. [b]Molecular environments including vacuum and chloroform. [c]Cost for planarization. [d]Energetic cost for flipping dihedral. [e]Barrier for rotation of dihedral.

of the CBB of each molecule using three values: planarization energy (E_p), the energy cost of flipping a dihedral from the optimized configuration (E_{fn}, where "n" is the bond defining the axis of rotation), and the energy barrier for dihedral rotation (E_{bn}). For all four isolated molecules, the geometry of the CBB at the energetic global minimum is congruent to the one chosen for illustration in Chart 1. It is important to point out that while these bonds can be assigned an orientation, due to sterics they do not necessarily adopt exactly 0 or 180° dihedral angles. However, because the planarization energies for these dihedrals are <10 meV at room temperature (see Table 1), all considered CBBs are statistically planar. Therefore, the conformational space of each CBB consists of $2^6 = 64$ rotational isomers, or rotamers. It is worth noting for the observed flipped dihedrals 1, 3, and 4 in crystal geometries of **3** and **4** that the E_{fn} energies are approximately at or below kT at 300 K. Dihedrals 3 and 4 in **1** and dihedrals 2 and 5 in **2** are trapped in a global minimum effectively locking their conformations. In the case of **1**, this would preclude adopting the geometry found in the crystal of **3**, or type *b*. Specific values for dihedral angles and energetic costs can be found in Tables S3−S6 in the Supporting Information for all 34 unique geometries of each molecule without aliphatic side groups.

dx.doi.org/10.1021/jz5012675 | J. Phys. Chem. Lett. 2014, 5, 2700−2704

Table 2. Summary of Computed Properties of Crystals Optimized by MM3 (Values Based on Observed Structures in Parentheses)

entry	conformation energy (eV)	binding energy (eV)	intrastack binding energy (eV)	interstack binding energy (eV)	exciton coupling (meV)	hole coupling (meV)
1a	0	3.39	2.04	0.45	65 (63)	53
1b	0.16	3.10	1.88	0.41	69	121
2a	0	3.28	2.06	0.41	45	40
2b	0.04	3.23	1.86	0.46	51	126
3a	0	2.99	2.08	0.30	57	65
3b	0.06	3.34	2.15	0.40	43 (30)	127
4a	0	3.14	2.06	0.36	65	44
4a′[a]	0	3.16	2.07	0.36	102 (113)	100
4a″[a]	0.02	3.18	2.02	0.39	80 (88)	75
4b	0.03	3.31	2.03	0.43	56 (46)	105

[a]4a′ and 4a″ represent experimentally determined crystal structures for **4** that adopt type *a* geometry, and prime and double prime accommodate two observed disorder contributions. Binding energies are reported per-molecule.

It should be noted that potential energy surfaces for the dihedrals of interest are sensitive to model chemistry (see Table S4 and Figure S6 in the Supporting Information). Despite the fact that our default ab initio method (CAM-B3LYP/6-31g*) was chosen to make valid comparisons with the available experimental data, the uncertainty of calculated differences in energies is larger than 10 meV (Figure S6 in the Supporting Information). Additionally, the difference in thermal vibrational energies between the most important rotamers does not exceed 10 meV, which is spread over the entire vibrational spectrum for a particular class of molecules. Therefore, we will neglect this contribution to energy. Finally, because we have a heteroatomic conjugated system, we have large atomic charges (Table S3 in the Supporting Information), and thus the rotamer energetics is sensitive to solvent.

As we previously mentioned, the huge conformational space of side chains may result in an important entropic contribution to rotamer energetics in solution. To address these issues, we employed MD calculations for a dynamic perspective and estimate of free energy. An interesting distinction between molecules **1** and **3** arises with the inclusion of side-chains regarding the barrier to rotation. Because of a favorable interaction between the aliphatic hydrogen atoms and the electronegative fluorine, side chains stabilize the rotation of dihedrals 3 and 4 from the lowest energy conformation in molecule **3**. This is seen in Figure S7 in the Supporting Information as a deviation between potential energy surface for dihedral 3 in CBB and free-energy surface for dihedral 3 in the full molecule.

After determining molecular conformational preferences in solution, we are now ready to analyze crystals. All experimentally determined structures of **1**−**4** have a common crystal motif: a closed-packed lattice of 1-D π-stacks. Figure 1 illustrates how cofacial neighbors arrange in the lattice for molecules **1** and **3** (Figure 1a,b, respectively). The CBB of all molecules in a single π-stack are perfectly aligned with typical $\pi-\pi$ stacking distance of 3.5 Å. All crystals have nearly the same molecular density (see Table S10 in the Supporting Information) while having very different microstructure, but all are consistent with the space filling being an important driving force for crystal formation. The key difference between the studied crystals is in the arrangement of molecules in a stack. From this perspective, only parallel and antiparallel stack types are observed, as determined by the mutual orientation of the neighboring molecules in a stack. An intrinsic static disorder, which is typical for crystals of such molecules, involves both side-chain and CBB conformations. To understand the lattice arrangements, we performed MM3 force-field calculations of the binding energies of molecules in a crystal (see Table 2). Here the static disorder is removed from the experimentally observed structure and then relaxed with MM3 force field. For system **4**, two conformations, 4a′ and 4a″, coexisting in a single crystal are considered separately. Among lattices not observed experimentally we consider only those corresponding to experimentally observed crystals **1** (type *a*) and **3** (type *b*). As expected, in all cases, calculated intrastack binding energy (∼2.0 eV/molecule) is much stronger than the interstack pairwise binding energy (∼0.4 eV/molecule). The latter is defined as the difference between the total and intrastack interaction energies divided by the number of interacting stack directions (three per stack).

The rationalization of the observed structural trends is straightforward based on conformation energy and intrastack and interstack binding energies from Table 2. For molecule **1**, all of the three components give a strong preference for the crystal structure observed experimentally (1a). For molecule **3**, the experimentally observed conformation 3b is not the lowest conformation in solution, but the energy difference, 60 meV, is small enough for this conformation to be populated at the room temperature. In addition, half of this energy is due to the rotation of the terminal thiophene, which, at a π-stack terminus would not have its rotation impeded by a cofacial π system (see Figure 1b). Intermolecular binding energies give a strong preference for the observed crystal structure (3b). For molecule **2**, the conformations 2a and 2b have even smaller energy difference in solution. The intrastack binding energy prefers the structure 2a, whereas the interstack interactions give preference to the structure 2b. We postulate that the frustration between the two polymorphs prevents single-crystal formation, and in fact we have not yet succeeded in the preparation of single crystals for this molecule. For molecule **4**, the experimentally observed conformations 4a′ and 4a″ are nearly isoenergetic in a solution. The intrastack binding energies are also nearly the same for each structure, and there is little variation in interstack energies. As a result, two polymorphs are observed for molecule **4** with the noticeable static disorder.

Molecular assembly in the discussed crystal motifs has profound implications on the materials electronic properties. To exemplify this statement, Table 2 shows exciton and hole in-stack nearest-neighbor intermolecular couplings computed by

dx.doi.org/10.1021/jz5012675 | J. Phys. Chem. Lett. 2014, 5, 2700−2704

DFT using previously reported methods.[15] Here we recall that hole mobility and exciton diffusion coefficient are roughly proportional to the squared couplings. While excitonic couplings are approximately similar for studied polymorphs, a clear trend is observed for hole couplings: type *b* crystal structure has two to three times larger coupling than type *a* structure owing to a better π-electronic overlap. This suggests much higher hole mobilities along the stack for type *b* crystals. A detailed study of excitons and charge transports in these materials will be reported in our future works.

In conclusion, we have used computational methods to reconcile disparate molecular packing arrangements for isostructural molecules that arise from seemingly innocent molecular features. The calculated rotational barriers and relative energies of different rotamers corroborate that in fact a diverse distribution of molecular species is likely to exist in a sample of material that exhibits this highly common form of asymmetry. Single-crystal structures indicate that an optimized molecular geometry cannot be assumed to represent a dominant species in the bulk or as the most likely candidate for single crystal formation. First-principle and dynamical calculations offer insight that is unavailable experimentally. This work assists in assessing key structural features of organic semiconductors more comprehensively, both retrospectively and moving forward. As this work is extended, one can envision an enhanced understanding on the mesoscopic scale and the possibility of a more ground-up approach to molecular design.

■ ASSOCIATED CONTENT

Supporting Information

Details of computational methods and supplemental calculations. This material is available free of charge via the Internet at http://pubs.acs.org.

■ AUTHOR INFORMATION

Corresponding Authors

*G.C.B.: E-mail: bazan@chem.ucsb.edu;
*S.T.: E-mail: serg@lanl.gov.

Notes

The authors declare no competing financial interest.

■ ACKNOWLEDGMENTS

We acknowledge support from the Institute for Collaborative Biotechnologies through grant W911NF-09-0001 from the U.S. Army Research Office. This work was also partially supported the U.S. Department of Energy and Laboratory Directed Research and Development (LDRD) program at Los Alamos National Laboratory (LANL). LANL is operated by Los Alamos National Security, LLC, for the National Nuclear Security Administration of the U.S. Department of Energy under contract DE-AC52-06NA25396. The Advanced Light Source is supported by the Director, Office of Science, Office of Basic Energy Sciences, of the U.S. Department of Energy under Contract No. DE-AC02-05CH11231.

■ REFERENCES

(1) Welch, G. C.; Perez, L. A.; Hoven, C. V.; Zhang, Y.; Dang, X.-D.; Sharenko, A.; Toney, M. F.; Kramer, E. J.; Nguyen, T.-Q.; Bazan, G. C. A Modular Molecular Framework for Utility in Small-Molecule Solution-Processed Organic Photovoltaic Devices. *J. Mater. Chem.* **2011**, *21*, 12700−12709.

(2) Dou, L.; You, J.; Hong, Z.; Xu, Z.; Li, G.; Street, R. A.; Yang, Y. 25th Anniversary Article: A Decade of Organic/Polymeric Photovoltaic Research. *Adv. Mater.* **2013**, *25*, 6642−6671.

(3) Cheng, Y.-J.; Yang, S.-H.; Hsu, C.-S. Synthesis of Conjugated Polymers for Organic Solar Cell Applications. *Chem. Rev.* **2009**, *109*, 5868−5923.

(4) Gendron, D.; Leclerc, M. New Conjugated Polymers for Plastic Solar Cells. *Energy Environ. Sci.* **2011**, *4*, 1225−1237.

(5) Henson, Z. B.; Welch, G. C.; van der Poll, T.; Bazan, G. C. Pyridalthiadiazole-Based Narrow Band Gap Chromophores. *J. Am. Chem. Soc.* **2012**, *134*, 3766−3779.

(6) Liu, J.; Mikhaylov, I. A.; Zou, J.; Osaka, I.; Masunov, A. E.; McCullough, R. D.; Zhai, L. Insight into How Molecular Structures of Thiophene-Based Conjugated Polymers Affect Crystallization Behaviors. *Polymer.* **2011**, *52*, 2302−2309.

(7) Hu, Z.; Liu, J.; Simón-Bower, L.; Zhai, L.; Gesquiere, A. J. Influence of Backbone Rigidness on Single Chain Conformation of Thiophene-Based Conjugated Polymers. *J. Phys. Chem. B* **2012**, *117*, 4461−4467.

(8) Lee, C. W.; Kim, O. Y.; Lee, J. Y. Organic Materials for Organic Electronic Devices. *J. Ind. Eng. Chem.* **2014**, *20*, 1198−1208.

(9) Bazan, G. C. Novel Organic Materials through Control of Multichromophore Interactions. *J. Org. Chem.* **2007**, *72*, 8615−8635.

(10) Vissenberg, M. C. J. M.; Matters, M. Theory of the Field-Effect Mobility in Amorphous Organic Transistors. *Phys. Rev. B* **1998**, *57*, 12964−12967.

(11) Horowitz, G. Organic Thin Film Transistors: From Theory to Real Devices. *J. Mater. Res.* **2004**, *19*, 1946−1962.

(12) Coropceanu, V.; Cornil, J.; da Silva, D. A.; Olivier, Y.; Silbey, R.; Bredas, J. L. Charge Transport in Organic Semiconductors. *Chem. Rev.* **2007**, *107*, 926−952.

(13) Wang, L. J.; Nan, G. J.; Yang, X. D.; Peng, Q.; Li, Q. K.; Shuai, Z. G. Computational Methods for Design of Organic Materials with High Charge Mobility. *Chem. Soc. Rev.* **2010**, *39*, 423−434.

(14) Bernstein, J. *Polymorphism in Molecular Crystals*; Oxford University Press: Oxford, U.K., 2002.

(15) Braga, D.; Grepioni, F.; Maini, L.; Polito, M. Crystal Polymorphism and Multiple Crystal Forms. *Struct. Bonding (Berlin, Ger.)* **2009**, *132*, 25.

(16) Davey, R. J.; Schroeder, S. L. M.; ter Horst, J. H. Nucleation of Organic Crystals−A Molecular Perspective. *Angew. Chem., Int. Ed.* **2013**, *52*, 2166.

(17) Liu, J.; Zhang, Y.; Phan, H.; Sharenko, A.; Moonsin, P.; Walker, B.; Promarak, V.; Nguyen, T.-Q. Effects of Stereoisomerism on the Crystallization Behavior and Optoelectrical Properties of Conjugated Molecules. *Adv. Mater.* **2013**, *25*, 3645.

(18) Price, S. L. Predicting Crystal Structures of Organic Compounds. *Chem. Soc. Rev.* **2014**, *43*, 2098.

(19) Olivier, Y.; Niedzialek, D.; Lemaur, V.; Pisula, W.; Mullen, K.; Koldemir, U.; Reynolds, J. R.; Lazzaroni, R.; Cornil, J.; Beljonne, D. 25th Anniversary Article: High-Mobility Hole and Electron Transport Conjugated Polymers: How Structure Defines Function. *Adv. Mater.* **2014**, *26*, 2119.

(20) Desiraju, G. R. Crystal Engineering: From Molecule to Crystal. *J. Am. Chem. Soc.* **2013**, *135*, 9952.

(21) Yang, D.; Yang, Q.; Yang, L.; Luo, Q.; Huang, Y.; Lu, Z.; Zhao, S. Novel High Performance Asymmetrical Squaraines for Small Molecule Organic Solar Cells with a High Open Circuit Voltage of 1.12 V. *Chem. Commun.* **2013**, *49*, 10465−10467.

(22) Huang, Y.-C.; Hsu, F.-H.; Cha, H.-C.; Chuang, C.-M.; Tsao, C.-S.; Chen, C.-Y. High-Performance Ito-Free Spray-Processed Polymer Solar Cells with Incorporating Ink-Jet Printed Grid. *Org. Electron.* **2013**, *14*, 2809−2817.

(23) Gupta, V.; Kyaw, A. K.; Wang, D. H.; Chand, S.; Bazan, G. C.; Heeger, A. J. Barium: An Efficient Cathode Layer for Bulk-Heterojunction Solar Cells. *Sci. Rep.* **2013**, *3*, 1965.

(24) Zhugayevych, A.; Postupna, O.; Bakus, R. C., II; Welch, G. C.; Bazan, G. C.; Tretiak, S. Ab Initio Study of a Molecular Crystal for

Photovoltaics: Light Absorption, Exciton and Charge Carrier Transport. *J. Phys. Chem. C* **2013**, *117*, 4920−4930.
(25) Love, J. A.; Proctor, C. M.; Liu, J.; Takacs, C. J.; Sharenko, A.; van der Poll, T. S.; Heeger, A. J.; Bazan, G. C.; Nguyen, T.-Q. Film Morphology of High Efficiency Solution-Processed Small-Molecule Solar Cells. *Adv. Funct. Mater.* **2013**, *23*, 5019−5026.
(26) Coughlin, J. E.; Zhugayevych, A.; Bakus, R. C.; van der Poll, T. S.; Welch, G. C.; Teat, S. J.; Bazan, G. C.; Tretiak, S. A Combined Experimental and Theoretical Study of Conformational Preferences of Molecular Semiconductors. *J. Phys. Chem. C* **2014**, DOI: 10.1021/jp506172a.
(27) Jackson, N. E.; Savoie, B. M.; Kohlstedt, K. L.; Olvera de la Cruz, M.; Schatz, G. C.; Chen, L. X.; Ratner, M. A. Controlling Conformations of Conjugated Polymers and Small Molecules: The Role of Nonbonding Interactions. *J. Am. Chem. Soc.* **2013**, *135*, 10475−10483.
(28) Jackson, N. E.; Savoie, B. M.; Kohlstedt, K. L.; Marks, T. J.; Chen, L. X.; Ratner, M. A. Structural and Conformational Dispersion in the Rational Design of Conjugated Polymers. *Macromolecules.* **2014**, *47*, 987−992.
(29) Lee, W.; Kim, G.-H.; Ko, S.-J.; Yum, S.; Hwang, S.; Cho, S.; Shin, Y.-H.; Kim, J. Y.; Woo, H. Y. Semicrystalline D−a Copolymers with Different Chain Curvature for Applications in Polymer Optoelectronic Devices. *Macromolecules.* **2014**, *47*, 1604−1612.
(30) Lee, J. B.; Kim, K. H.; Hong, C. S.; Choi, D. H. High-Performance Amorphous Donor−Acceptor Conjugated Polymers Containing X-Shaped Anthracene-Based Monomer and 2,5-Bis(2-Octyldodecyl)Pyrrolo[3,4-C]Pyrrole-1,4(2h,5h)-Dione for Organic Thin-Film Transistors. *J. Polym. Sci., Part A: Polym. Chem.* **2012**, *50*, 2809−2818.
(31) Zheng, N.; Li, H.; Sun, G.; Zhong, K.; Yin, B. Synthesis and Properties of T-Shaped Organic Conjugates Based on 3,6-Diarylpyridazine-Fused Tetrathiafulvalene. *Org. Biomol. Chem.* **2013**, *11*, 5100−5108.
(32) Zhou, J.; Wan, X.; Liu, Y.; Long, G.; Wang, F.; Li, Z.; Zuo, Y.; Li, C.; Chen, Y. A Planar Small Molecule with Dithienosilole Core for High Efficiency Solution-Processed Organic Photovoltaic Cells. *Chem. Mater.* **2011**, *23*, 4666−4668.
(33) Diallo, A. K.; Metri, N.; Brunel, F.; Sallenave, X.; Goubard, F.; Margeat, O.; Ackermann, J.; Videlot-Ackermann, C. A Star-Shaped Molecule as Hole Transporting Material in Solution-Processed Thin-Film Transistors. *Synth. Met.* **2013**, *184*, 35−40.
(34) Yum, S.; An, T. K.; Wang, X.; Lee, W.; Uddin, M. A.; Kim, Y. J.; Nguyen, T. L.; Xu, S.; Hwang, S.; Park, C. E.; et al. Benzotriazole-Containing Planar Conjugated Polymers with Noncovalent Conformational Locks for Thermally Stable and Efficient Polymer Field-Effect Transistors. *Chem. Mater.* **2014**, *26*, 2147−2154.
(35) Sugita, Y.; Okamoto, Y. Replica-Exchange Molecular Dynamics Method for Protein Folding. *Chem. Phys. Lett.* **1999**, *314*, 141−151.
(36) Kwon, S.; Wee, K.-R.; Kim, J. W.; Pac, C.; Kang, S. O. Effects of Intermolecular Interaction on the Energy Distribution of Valance Electronic States of a Carbazole-Based Material in Amorphous Thin Films. *J. Chem. Phys.* **2012**, *136*, 204706.
(37) Gring, M.; Gerlich, S.; Eibenberger, S.; Nimmrichter, S.; Berrada, T.; Arndt, M.; Ulbricht, H.; Hornberger, K.; Müri, M.; Mayor, M.; et al. Influence of Conformational Molecular Dynamics on Matter Wave Interferometry. *Phys. Rev. A* **2010**, *81*, 031604.
(38) Filatov, M. Assessment of Density Functional Methods for Obtaining Geometries at Conical Intersections in Organic Molecules. *J. Chem. Theor. Comput.* **2013**, *9*, 4526−4541.
(39) Balamurugan, D.; Aquino, A. J. A.; de Dios, F.; Flores, L.; Lischka, H.; Cheung, M. S. Multiscale Simulation of the Ground and Photo-Induced Charge-Separated States of a Molecular Triad in Polar Organic Solvent: Exploring the Conformations, Fluctuations, and Free Energy Landscapes. *J. Phys. Chem. B* **2013**, *117*, 12065−12075.